ENGINEERING

Singlet-filtered NMR spectroscopy

Salvatore Mamone[1,2]*, Nasrollah Rezaei-Ghaleh[3,4], Felipe Opazo[2,5], Christian Griesinger[4], Stefan Glöggler[1,2]*

Selectively studying parts of proteins and metabolites in tissue with nuclear magnetic resonance promises new insights into molecular structures or diagnostic approaches. Nuclear spin singlet states allow the selection of signals from chemical moieties of interest in proteins or metabolites while suppressing background signal. This selection process is based on the electron-mediated coupling between two nuclear spins and their difference in resonance frequency. We introduce a generalized and versatile pulsed NMR experiment that allows populating singlet states on a broad scale of coupling patterns. This approach allowed us to filter signals from proton pairs in the Alzheimer's disease–related β-amyloid 40 peptide and in metabolites in brain matter. In particular, for glutamine/glutamate, we have discovered a long-lived state in tissue without the typically required singlet sustaining by radiofrequency irradiation. We believe that these findings will open up new opportunities to study metabolites with a view on future in vivo applications.

INTRODUCTION

Nuclear magnetic resonance (NMR) is a technique that has influenced the field of structural biology and biomedicine. With respect to the former, new NMR-based techniques allow for better insights into protein structures and dynamics (*1*). Regarding the field of biomedicine, the advancement of NMR leads not only to improved diagnostic tools but also to a better understanding of biological processes in vivo (*2*). Here, we demonstrate an NMR method for filtering signals of glycine residues in an Alzheimer-related protein [β-amyloid 40 (Aβ40)] and to probe specific metabolites in brain matter. The main benefit that we are going to present here is that an unwanted background from omnipresent protons is suppressed. For protein investigations, this offers opportunities to analyze structural properties at certain positions without the need for isotopic labeling strategies. Furthermore, we are paving the pathway for new metabolite investigations in the brain tissue as proton signals, including water, are sufficiently suppressed, while the signals of certain metabolites are retained. Because of the abundance of metabolites in brain tissue, signals of interest may often be masked and inaccessible.

The developments presented here rely on the phenomenon of nuclear spin singlet states. Singlet states are effective spin-0 states that can be formed in homonuclear spin-½ pairs and detected indirectly, despite being NMR silent (*3*, *4*). One special feature of these states is that the characteristic lifetime (T_S) is, in many cases, longer than the characteristic recovery time for the longitudinal magnetization to return to its thermodynamical equilibrium state (T_1) (*3*). Several relaxation mechanisms, which act as strong relaxation sources for magnetization, are ineffective for singlet states (*5*). Nuclear spin singlet states have been explored over the past years for a variety of applications. One research goal with relevant implications for clinical magnetic resonance imaging (MRI) is to preserve nuclear spin hyperpolarization (*6*–*12*). Hyperpolarization methods can transiently enhance NMR signals by more than four orders of magnitude leading to large gains in sensitivity (*13*–*17*). Hyperpolarized magnetization decays within T_1 but may be preserved for longer times if stored in a singlet state (*6*–*12*). T_S of more than 1 hour was observed so far (*10*), and molecules in which hyperpolarization can be maintained for a long period of time have been proposed to be used as biosensors (*11*, *12*). Singlet NMR has also been used for the investigation of dynamic phenomena. Because of long T_S as compared to T_1, translational diffusion coefficients of molecules can be determined on a longer time scale (*18*), and the singlet state can be used to probe drug binding with improved precision (*19*). Singlet states have furthermore been used to investigate the folding of proteins (*20*, *21*), self-assembling phenomena (*22*), or as stimuli-responsive probes in synthetic macromolecules (*23*). Last, singlet states can be used to filter out certain resonances from undesired background signals (*22*, *24*).

Over the years, several NMR sequences were invented to access singlet states (*3*, *4*, *8*, *18*, *24*–*27*). The available sequences generally tend to perform better in some spin systems than in others depending on spin couplings and on off-resonance effects of the pulses. For example, the M2S (*8*) sequence and the sequence introduced by Sarkar *et al.* (*18*) are offset independent, but their use is limited to a strongly coupled and a weakly coupled spin system, respectively. Strongly coupled means that the electron-mediated coupling (*J*-coupling) between two spins is larger than the difference in chemical shift, whereas weakly coupled represents the opposite case. The SLIC (Spin-Lock-Induced Crossing) sequence (*28*) has been demonstrated for strongly coupled spin systems and suffers from offset dependence. Last, the APSOC (Adiabatic Passage Singlet Order Conversion) sequence (*24*, *25*) is applicable to a weakly and strongly coupled spin system, but it requires relatively stringent conditions on the offset of the conversion pulses. When a sequence is sensitive to the carrier frequency of the radio frequency (RF) pulses, its robust application can be compromised, e.g., in in vivo imaging studies where movements of the subject of interest and concomitant resonance shifts may negatively affect the whole experiment. It appears desirable to have one single offset independent pulse sequence capable of populating singlet states in all possible coupling regimes from strongly to weakly coupling, including the intermediate regime. Here, we demonstrate a sequence

[1]NMR Signal Enhancement Group, Max Planck Institute for Biophysical Chemistry, AmFaßberg 11, 37077 Göttingen, Germany. [2]Center for Biostructural Imaging of Neurodegeneration of UMG, Von-Siebold-Straße 3A, 37075 Göttingen, Germany. [3]Department of Neurology, University Medical Center Göttingen, Waldweg 33, 37073 Göttingen, Germany. [4]Department for NMR-based Structural Biology, Max Planck Institute for Biophysical Chemistry, Am Faßberg 11, 37077 Göttingen, Germany. [5]Institute for Neuro- and Sensory Physiology, University Medical Center Göttingen, Humboldtallee 23, 37073 Göttingen, Germany.
*Corresponding author. Email: salvatore.mamone@mpibpc.mpg.de (S.M.); stefan.gloeggler@mpibpc.mpg.de (S.G.)

that can populate singlet states in all coupling regimes in systems as complex and dynamic as Alzheimer-related proteins and in specific metabolites in intact nonhomogenized brain matter. In the investigated case of glutamate in brain matter, we have discovered a long-lived state. In particular, the latter represents the proof that long-lived states can be detected in tissue and hence substantially broadens opportunities for future biomedical applications.

RESULTS

Introducing the general coupling magnetization-to-singlet (gc-M2S) experiment

In this section, we briefly discuss the sequence with all the necessary details to perform the experiment. A more detailed discussion of the theory can be found in the Supplementary Materials.

The aim of any singlet sequence is to convert magnetization into singlet states and back. To this scope, three blocks are required: a first block for generating singlet order from magnetization (magnetization to singlet), a second block to suppress the nonsinglet character of the spin density operator (abbreviated as T_{00} filter), and a final block to convert the singlet back into observable magnetization (singlet to magnetization) (see Fig. 1). Other additional blocks, such as the depicted z-purge and/or water suppression, can be used to record clean in-phase signals but are not essential. The various singlet sequences differ on the substructure of the blocks, which ultimately determines the operator route in exciting and reconverting singlet states.

The innovation of the sequence proposed here lies in the fact that it works for both strongly and weakly coupled spin systems, as well as in the intermediate range in an offset independent manner as M2S. It therefore adds to M2S that it does not require strong coupling between the spins from which the singlet state is populated. In particular, we show here that by defining the basic echoes and their durations in single quantum (SQ) blocks and by matching the delays in the zero quantum (ZQ) block on the basis of the exact dynamics of the coupled spin system, it is possible to create singlets in any arbitrary coupled regime. We propose the acronym gc-M2S (general coupling magnetization to singlet) (see Fig. 1). Below, we give a brief description of the sequence and the related spin dynamics.

In an isolated homonuclear spin-½ pair placed in a magnetic field, the isotropic liquid-state nuclear spin Hamiltonian (in units of the Planck reduced constants $\hbar$) has the form

$$H = \underbrace{\omega_\Sigma(I_{1z}+I_{2z})/2}_{H_0} + \underbrace{\omega_\delta(I_{1z}-I_{2z})/2 + 2\pi J_{12}\boldsymbol{I}_1\cdot\boldsymbol{I}_2}_{H_1} \quad (1)$$

where J_{12} is the scalar J-coupling in hertz and $\omega_\Sigma = (\omega_1 + \omega_2)$ and $\omega_\delta = (\omega_1 - \omega_2)$ are the sum and difference of the chemical shifts between the two spins in radians per second, respectively. The parameter

$$\varepsilon = \omega_\delta/(2\pi J_{12}) \quad (2)$$

determines whether the spin system is in the strong ($|\varepsilon| < 0.2$), weak ($|\varepsilon| > 5$), or intermediate ($0.2 \leq |\varepsilon| \leq 5$) coupling regime.

In typical NMR or MRI experiments, the initial spin density operator for an isolated spin-½ pair is well approximated by the thermal equilibrium operator $\rho_T \propto (I_{1z} + I_{2z})/2$, where the proportionality factor is given by the thermal polarization, which is implied henceforth. The first $(\pi/2)_{\phi 1}$ pulse rotates the initial thermal equilibrium state, which corresponds to magnetization aligned along the external magnetic field into magnetization in the transverse plane. In the $M2S_{SQ}$ block (Fig. 1), a train of n_1 echoes in the form $\tau - \pi - \tau - \pi$, where π represents a π-pulse and

$$\tau = 1/\left[2\sqrt{J_{12}^2 + \left(\frac{\omega_\delta}{2\pi}\right)^2}\right] \quad (3)$$

followed by a second $(\pi/2)_{\phi 2}$ pulse, partly converts the initial operator to useful ZQ order. The phase ϕ_2 is in quadrature with respect to phase ϕ_1 and the amplitude is given by $f_{SQ}^{M2S}(n_1) = |\sin(n_1\theta_1)|$, where $\theta_1 = 2\arctan\left(\frac{1}{\varepsilon}\right)$. The aim of the $M2S_{SQ}$ block is to maximize f_{SQ}^{M2S} by setting an appropriate number of echoes n_1. A quasi-optimal choice of echoes is given by

$$\bar{n}_1(\varepsilon) = \begin{cases} \text{Round}\left[\dfrac{\pi}{4\arctan(|\varepsilon|)}\right] & 0 < |\varepsilon| < 1/\sqrt{3} \\ 1 & 1/\sqrt{3} \leq |\varepsilon| \leq \sqrt{3} \\ \text{Round}\left[\dfrac{\pi}{4\arctan(1/|\varepsilon|)}\right] & |\varepsilon| > \sqrt{3} \end{cases} \quad (4)$$

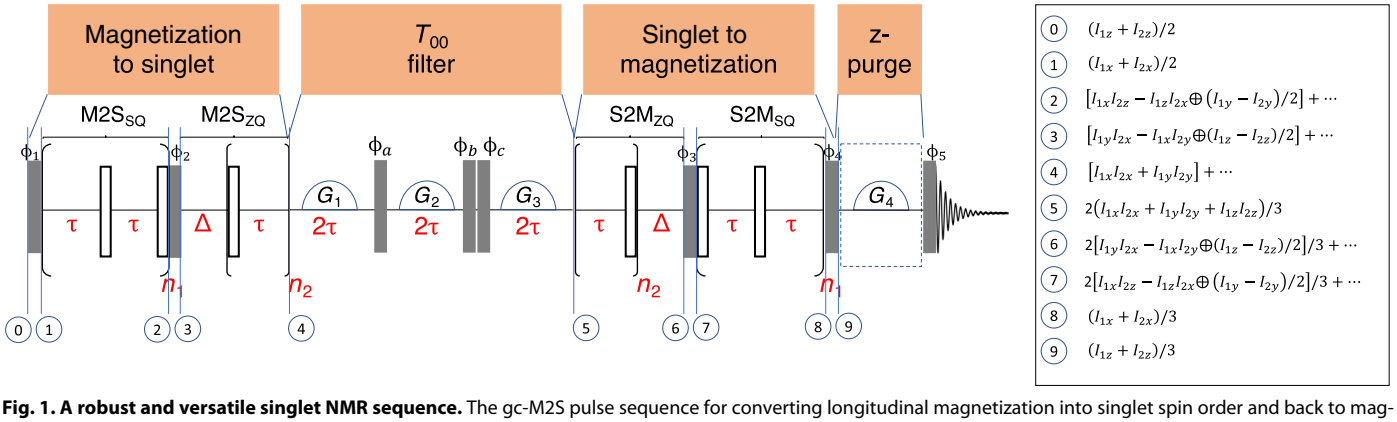

Fig. 1. A robust and versatile singlet NMR sequence. The gc-M2S pulse sequence for converting longitudinal magnetization into singlet spin order and back to magnetization in a homonuclear 2 spin-½ system is shown. Full and empty rectangles represent $\pi/2$ and π hard pulses, respectively, and the semicircles represent gradients. The sequence consists of a magnetization-to-singlet block, a T_{00} block to project into the singlet state, a singlet-to-magnetization block, a z-purge block, and a $(\pi/2)_{\phi_5}$ observe block. The phases ϕ_1 and ϕ_4 are collinear. The phases ϕ_2 and ϕ_3 are collinear but in quadrature to ϕ_1 and ϕ_4. The relevant product operators of each step are given on the right. The detailed discussion can be found in the Supplementary Materials.

With regard to the spin dynamics during the $M2S_{ZQ}$ block (Fig. 1), the evolution of the relevant operators is restricted to the three-dimensional Liouville subspace spanned by the ZQ operators $\{ZQ_x = I_{1x}I_{2x} + I_{1y}I_{2y}, ZQ_y = I_{1y}I_{2x} - I_{1x}I_{2y}, ZQ_z = (I_{1z} - I_{2z})/2\}$. In this subspace, the free evolution corresponds to a rotation along an axis with coordinates proportional to {1,0, ε}, and angular frequency $\omega_{ZQ} = \pi/\tau$. The block $[\pi - \tau]$ is equivalent to a rotation along the ZQ_y axis in the ZQ_{zx} plane by an angle $\theta_2 = -2 \arctan(\varepsilon)$. The aim of the $M2S_{ZQ}$ block is to maximize the projection along ZQ_x of the operator created by the previous part of the sequence. This is achieved by selecting an appropriate delay to bring the initial ZQ operator from the *zy* plane into the *zx* plane and then to repeat the block $[\pi - \tau]$ n_2 times to drive the evolved operator as close as possible to the *x* axis. The orbit of the initial operator crosses the *zy* plane at delays $\overline{\Delta}$

$$\overline{\Delta}/\tau = \mathrm{Mod}\left[\arctan\frac{1}{\rho\tan(\pi\,\overline{n}_1\rho)}, \pi\right] \quad (5)$$

where $\rho = \frac{1}{\left(\sqrt{1+\varepsilon^2}\right)}$. The choice

$$\overline{n}_2(\varepsilon) = \begin{cases} \overline{n}_1(\varepsilon) - 1 & 0 < |\varepsilon| \leq 0.4 \\ 1 & 0.4 < |\varepsilon| \leq 0.7 \\ 0 & 0.7 < |\varepsilon| \leq 2.5 \\ 1 & 2.5 < |\varepsilon| \leq 2\pi \\ \mathrm{Round}\left[\frac{\varepsilon}{\pi}\right] & |\varepsilon| > 2\pi \end{cases} \quad (6)$$

provides a compromise between keeping a small number of echoes and maintaining an acceptable transfer efficiency. Further details can be found in the Supplementary Materials.

The state obtained at the end of the magnetization-to-singlet block is channeled into the singlet state by the T_{00}-pass filter represented in Fig. 1. The filter alternates gradients and 90° flip pulses. With a choice of gradients that ensures linearly independent accumulated phases, only ZQ operators need to be considered in the discussion of the filter. The block G_1-pulse-G_2 suppresses odd-rank ZQ spherical tensors, and the block G_2-pulse-G_3 suppresses the rank-2 ZQ operator (*29*). Each block duration is matched to a multiple of 2τ to ensure that the component proportional to the singlet operator is fully recovered at the terminal points of the corresponding free evolution period (*29*). The singlet-to-magnetization block acts in reverse of the magnetization-to-singlet block so that the ZQ_x component of the singlet state operator retraces backward, closely but not exactly, the path discussed for the magnetization-to-singlet block. After the pulse $(\pi/2)_{\phi_4}$, residual undesired operators present at the end of the block are removed by the z-purge section.

The maximum efficiency for magnetization-to-singlet-to-magnetization conversion has an upper bound of 2/3 (*30*). The gc-M2S sequence can achieve the theoretical upper bound asymptotically in the limit of strong ($\varepsilon \to 0$) and weak ($\varepsilon \to \infty$) coupling. In general, the efficiency remains above 40% outside the strong and weak coupled limit ($|\varepsilon| < 0.2$ and $|\varepsilon| > 5$). The lowest efficiency is about 40%, found at $|\varepsilon| = 1/\sqrt{3}$ and $|\varepsilon| = \sqrt{3}$. We have proven this via simulations and show high experimental conversion efficiency in typical molecules bearing relatively isolated ^{1}H pairs as discussed in the Supplementary Materials.

In summary, the gc-M2S sequence achieves magnetization-to-singlet conversion by targeting the set of useful operators $I_{1x}I_{2z} - I_{1z}I_{2x}$ and $(I_{1y} - I_{2y})/2$ and reducing the conversion to $I_{1y}I_{2z} + I_{1z}I_{2y}$ at the end of the SQ block (see Fig. 1). For spin system in the near-equivalent regime, the gc-M2S reaches the singlet state via the operator $I_{1y}I_{2x} - I_{1x}I_{2y}$ rather than via $(I_{1y} - I_{2y})/2$ as in the M2S sequence (*31*).

Selective detection of multiple glycine-related singlets in Aβ peptide

To investigate the applicability of the gc-M2S experiment in complex systems, we turned our attention to Aβs, which are 39- to 43-residue peptides that aggregate into amyloid plaques in Alzheimer's disease (AD). Aβ40 is the main component of amyloid plaques in AD brains. The monomeric Aβ40 peptide undergoes extensive dynamics at multiple time and length scales and therefore samples a highly heterogeneous ensemble of conformations, typical of intrinsically disordered proteins. Consequently, the dispersion in the NMR chemical shifts of its amino acid residues is rather limited, and the NMR spectra are usually crowded (figs. S6 and S10).

In Aβ40, there are six glycines, G9, G25, G29, G33, G37, and G38. The Aβ glycines are located within the peptide regions, which are potentially important for the function and/or toxic aggregation of Aβ. For example, G9 is preceded by S8, a site of phosphorylation potentially linked to the progression of AD (*32*, *33*), and G25 and G29 are close to S26 whose phosphorylation interferes with the Aβ fibrillar aggregation (*34*). It has also been suggested that G37 and G38 are involved in the turn formation in the C-terminal region, where its stabilization in the C-terminally extended Aβ42 variant probably plays a role in the higher propensity of Aβ42 to toxic aggregation (*35*). On this background, it is highly desirable to develop NMR probes for monitoring these individual glycines located within the key regions of the Aβ peptide.

The H_α pairs of the six glycines of Aβ40 exhibit different levels of "apparent" splitting: G9, G33, and G38 show fairly large splitting of the two H_αs, while no apparent splitting is observed for G25, G29, and G37 (Fig. 2). The differential splitting of various glycines makes Aβ a suitable candidate to demonstrate the capability of the pulse sequence. Within the weak-coupling regime, we could fairly easily select for the H_α pairs of G38 and G33, separately (Fig. 2). The spectrum of G38 showed additional peaks belonging to G9. This is probably due to the similar ε ratios of G38 and G9, which compromises their selective recovery through the pulse-echo series. The used parameter values are consistent with the ε ratio order of G38 ~ G9 < G33. On the other hand, setting the sequence parameters within the range suitable for the strong-coupling regime, the H_αs of G25, G29, and G37 were resolved. The ε ratio order is G37 < G29 < G25. Overall, all the six glycines of Aβ40 could be detected. These results demonstrate that the method presented here can select different glycines on the basis of variations in the spin system parameters, even in systems as complex and dynamic as the Aβ peptides. To prove that only the desired glycines are observed, we have performed singlet-filtered total correlation spectroscopy (TOCSY) experiments in H_2O. We succeeded in observing four of the desired glycine protons coupled to their amide NH moieties in H_2O (Fig. 2B). The HA-HN cross peaks of G9 and G25 were not observed, probably due to low signal-to-noise ratio. They are, however, observable in singlet-filtered one-dimensional (1D) spectra measured in H_2O (fig. S8) despite coupling to an exchangeable HN proton.

Selective detection of metabolites in the brain

As a further application, we are going to show that certain metabolite signals can be filtered against a proton-rich tissue background in brain matter. Singlet states were excited in three representative

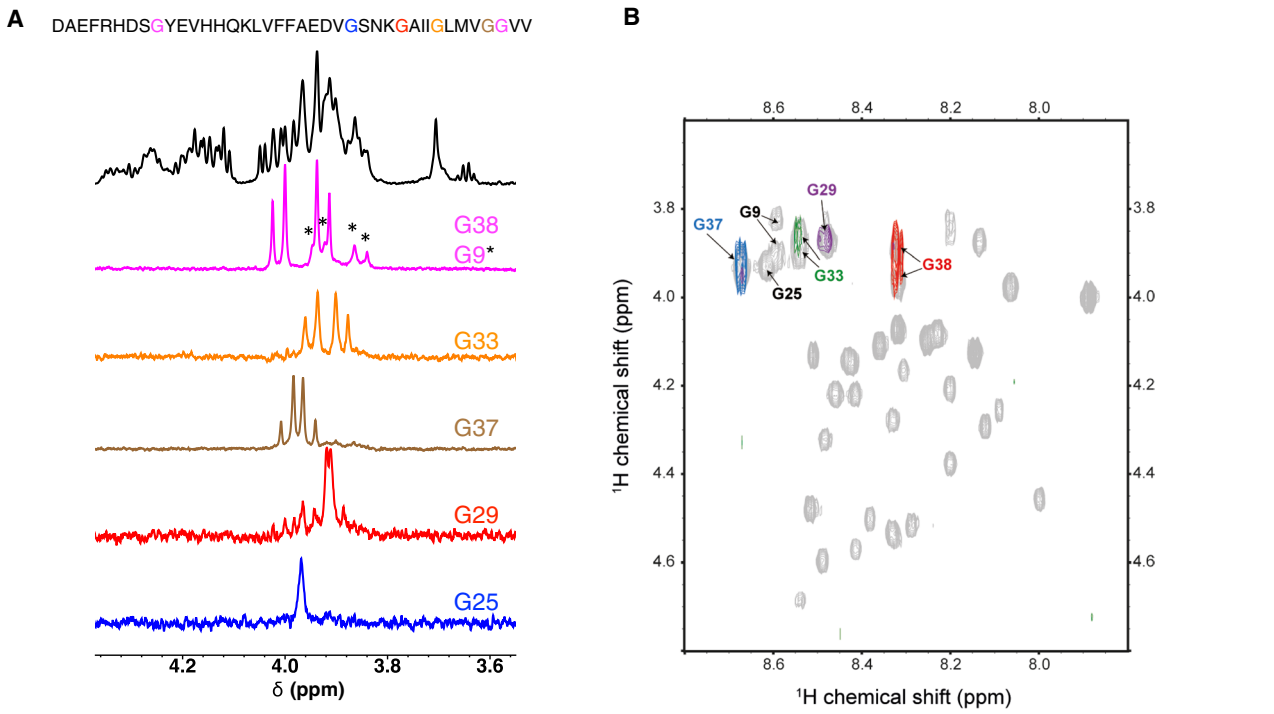

Fig. 2. Filtering signals in Aβ. ^{1}H NMR spectroscopy of glycine residues in Aβ40 at 278 K in a 16.48-T (700-MHz) magnet. (**A**) From top to bottom: Amino acid sequence and 1D-NMR ^{1}H (in black) and singlet-filtered spectra (in colors) for a 95 μM Aβ40 in D_2O. (**B**) Two-dimensional NMR ^{1}H-^{1}H correlation spectroscopy for a 95 μM Aβ40 in (90%/10%) H_2O/D_2O: TOCSY (60 ms mixing time, gray contours) with overlaid singlet-filtered TOCSYs (45 ms mixing time) using sequence parameters selective for G29 (purple contour), G33 (green contours), G37 (blue contours), and G38 (red contours), respectively. Full spectra are presented in the Supplementary Materials.

brain metabolites: glutamate (Glu), glutamine (Gln), and *N*-acetyl aspartate (NAA). Glutamate, glutamine, and NAA are among the molecules with highest concentrations, ~2 to 10 mM, in the human brain and play a fundamental role in several processes and metabolic cycles occurring in the normal as well as in altered states of the brain (*36*, *37*). ^{1}H MRI of the brain suffers from spectral superposition and broadening effects (*38*) and singlet-filtered sequences may come useful to unravel complexity and achieve metabolite quantification (*39*). As demonstrated in Fig. 3, the parameters of the gc-M2S sequence can be tuned to highlight the gamma protons of Glu and Gln, collectively labeled as Glx, and the beta protons in NAA while removing the signals from other endogenous molecules. The parameters defining the spin systems in Glx and NAA are sufficiently different (*40*) to allow selective excitation of the singlet-filtered signal via the gc-M2S sequence. Figure 3 collects a set of experiments on ex vivo intact mouse brains. In the ^{1}H NMR spectra of the mouse brains (bottom trace of Fig. 3A), there is a strong overlap of the resonances, and direct spectral assignment and quantification are complicated except for the sharpest and most intense resonances. These include the methyl signal from lactate [1.33 parts per million (ppm)] and NAA (2.03 ppm). Other important resonances include creatine (3.00 ppm) and choline (3.22 ppm). Metabolite quantification is also compounded by line-broadening effects, originating from relatively poor homogeneity in the given experimental conditions. However, the singlet-filtered experiments in Fig. 3A reveal the spectral signatures of the H_γ pair in Glx and the H_β pair in NAA. Last, we notice that although possible, no singlet sustaining block was used to enhance signal selectivity. Singlet sustaining requires irradiating on-resonance with a pulse several times stronger than the chemical shift difference between the two spins, and the resulting power deposition effects may be unfavorable for in vivo applications.

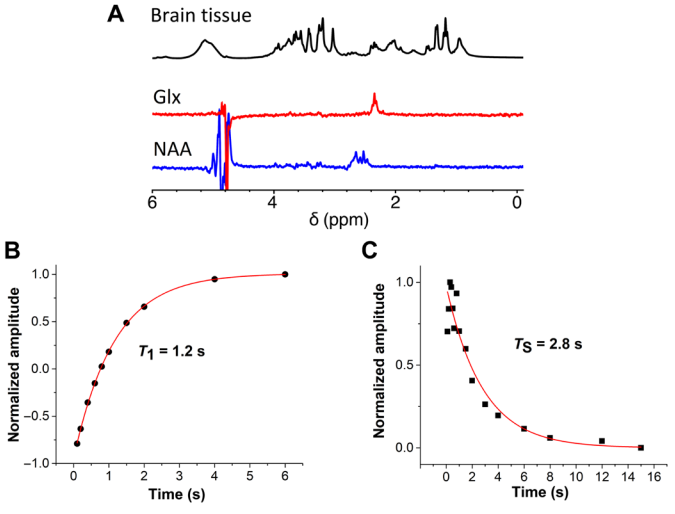

Fig. 3. Analyzing metabolites in the brain via singlet states. (**A**) Top to bottom: the ^{1}H NMR spectrum of ex vivo mouse brains (128 scans, spectrum is divided by 32) and the corresponding singlet-filtered NAA_β and Glx_γ spectra (128 scans, acquisition time ~3 min). In all the spectra, a polynomial pulse sequence was appended for water suppression. All experiments have been conducted at 7.05 T (300 MHz). The experimental parameters for the sequence are reported in table S4. The composition of the buffer is reported in the Supplementary Materials. (**B**) T_1 of the Glx signal and (**C**) T_S, displaying long-lived behavior.

Signal filtration allows estimating relaxation times of the selected proton pairs in the excised mouse brains. In particular, we have further

investigated Glx at 7.05 T and found a longitudinal relaxation time of the gamma protons of $T_1(H_\gamma)$ = 1.2 s (Fig. 3B). Determining this time was made possible by combining the gc-M2S experiment with an inversion recovery experiment that suppresses all of the resonances in the spectrum of the brain and allows for a clean determination of T_1. The estimated singlet lifetime of Glx in brain matter is $T_S(H_\gamma)$ = 2.8 s (Fig. 3C) without applying sustaining RF pulses during the evolution period between the singlet excitation and reconversion block. The value of T_S without sustaining is an estimate of the ZQ coherence lifetime, as oscillations are not negligible at small delay, but as shown in Fig. 3C, the singlet-filtered signal is a long-lived state.

DISCUSSION

Overall, we have introduced a versatile pulsed NMR experiment, termed gc-M2S, that allows for accessing nuclear spin singlet states in homonuclear spin pairs over a broad range of coupling regimes. Using this experiment, we have filtered signals of glycine residues in Alzheimer-related Aβ40 while suppressing other undesired proton resonances. Moreover, we show the first successful singlet NMR experiment conducted in tissue. In brain matter, we succeeded in filtering specific metabolites including glutamine/glutamate and *N*-acetyl aspartate that may be obscured by other signals present. In addition, we have discovered a long-lived state in glutamine/glutamate signals in tissue without RF sustaining of the singlet state. The overall applicability of the sequence spans from strongly coupled to weakly coupled spin systems including the intermediate coupling region, making it a versatile tool for a variety of applications. In addition, the NMR experiment is independent of the offset, which makes it a robust sequence to be used in applications such as structural biology or MRI. When the average frequency of the two spins may fluctuate, the offset independence of the gc-M2S sequence is highly advantageous. On one hand, a fluctuation in frequency is observed during in vivo MRI studies due to, e.g., breathing motion. On the other hand, this is encountered for instance in some intrinsically disordered peptides and proteins such as Aβ, where intra- and intermolecular conformational exchange processes occur over a broad range of time scales. All of the above-described advantages demonstrate the viability for using singlet states in structural biology and biomedical investigation. We especially envision that singlet state experiments will become possible in vivo and in a first instance be used to study metabolism and metabolic dysfunction in the future.

MATERIALS AND METHODS

Amyloid-β peptide 40

Aβ40 was synthesized through solid-phase chemical synthesis. To dissolve the preformed aggregates of Aβ, the Aβ was treated with 20 mM NaOH or NaOD before bringing to the final solution (20 mM protonated or deuterated sodium phosphate, pH or pD of 7.4). In both samples, the final concentration of Aβ40 was 0.4 mg/ml, ca. 95 μM.To avoid peptide aggregation, all NMR experiments of Aβ40 were performed at 278 K.

The standard $^1H,^1H$ TOCSY spectrum of Aβ40 was acquired using the DIPSI2 (Decoupling In the Presence of Scalar Interactions) mixing sequence with an RF field strength of 10 kHz for 60 ms and 512 t_1 increments. In singlet-filtered TOCSY experiments, frequency labeling of glycine H_α pairs was achieved using 128 t_1 increments after selection for the singlet state of specific glycines using parameters listed in table S3. Then, a DIPSI2 mixing sequence with an RF field strength of 10 kHz and a duration of 45 ms transferred magnetization to the coupled amide protons before signal acquisition.

Brain experiments

Postnatal (P1 to P2) pups from a Wistar rat were decapitated with sterile scissors, and heads were placed on a sterile petri dish under a dissecting microscope. Using small sterile scissors, the cranium of each pup was opened from the back of the neck to the nose by inserting one tip of the scissors into the vertebral foramen and then proceeding anteriorly. Entire brains were then carefully removed from the skull with forceps and placed on ice-cold sterile Hanks' balanced salt solution (Sigma-Aldrich). The cerebellums were removed with a scalpel, and the two hemispheres were separated. Cerebellum-free brain halves were then transferred into Gibco phosphate-buffered saline buffer (pH 7.4) 1× (Thermo Fisher Scientific, 10010023) (155.17 mM NaCl, 2.97 mM Na_2HPO_4-$7H_2O$, and 1.06 mM KH_2PO_4). Approximately 20 cerebellum-free brains were loaded in a 10-mm NMR glass tube for measurements, occupying about 3 cm^3.

Instrumentation

The following NMR spectrometers were utilized to carry out the described experiments:

(1) A 7.05-T (300-MHz ^1H Larmor frequency) superconducting magnet equipped with inverse double-resonance room-temperature probes (PA BBO BB-H-D with Z gradient, 5 and 10 mm) and AVANCE III-HD console. Typical 90° pulse lengths were 9 μs for the 5-mm probe and 26 μs for the 10-mm probe.

(2) A 16.48-T (700-MHz ^1H Larmor frequency) superconducting magnet equipped with an inverse triple resonance cryo-probe (CPP TCI H&F-C/N-D-05 with Z gradient) and AVANCE III-HD console. Typical 90° pulse lengths were 7.5 μs.

SUPPLEMENTARY MATERIALS

Supplementary material for this article is available at http://advances.sciencemag.org/cgi/content/full/6/8/eaaz1955/DC1

Supplementary information

Fig. S1. The plot represents the $M2S_{SQ}$ transfer function $f_{SQ}^{M2S}(\bar{n}_1) = |\mathrm{Sin}\,\bar{n}_1\theta_1|$, where $\bar{n}_1(\varepsilon)$ is given in Eq. 4.

Fig. S2. Dependence of ε of the sequence parameters and transfer function.

Fig. S3. The numerical simulation illustrates the spin dynamics during the core magnetization-to-singlet and singlet-to-magnetization blocks.

Fig. S4. NMR spectra and singlet filtering of model compounds at various magnetic fields.

Fig. S5. The influence of the offset on the NMR signal passing through the gc-M2S sequence was evaluated in experiments on AGG at 21.15 T (900 MHz).

Fig. S6. ^1H NMR spectrum of Aβ40 in D_2O at 16.48 T (~700 MHz) and 278 K using a polynomial sequence for water suppression.

Fig. S7. ^1H NMR singlet-filtered spectra of Aβ40 in D_2O at 16.48 T (~700 MHz) and 278 K using the sequence of Fig. 1 with the parameters reported in table S3 to achieve selectivity for each glycine residue.

Fig. S8. ^1H NMR singlet-filtered spectra of Aβ40 in H_2O/D_2O (90%/10%) at 16.48 T (~700 MHz) and 278 K using the sequence of Fig. 1 with the parameters reported in table S3 to achieve selectivity for each glycine residue.

Fig. S9. TOCSY spectrum of Aβ40 in H_2O/D_2O (90%/10%) 16.48 T (~700 MHz) and 278 K obtained using a 60-ms DIPSI2 (ω_{RF} = 10 kHz) mixing block.

Fig. S10. Singlet-filtered TOCSYs spectra of Aβ40 in H_2O/D_2O (90%/10%) at 16.48 T (~700 MHz) and 278 K obtained using a 45-ms DIPSI2 (ω_{RF} = 10 kHz) mixing block.

Fig. S11. Tissue control experiments.

Table S1. The table reports the constants defining the nuclear spin Hamiltonian as well as the parameters used to set the GE-M2S sequence in the experiments on the H_2N-AlanylGlycilGlycine-OH (AGG) peptide presented in figs. S4 (B to D) and S5.

Table S2. The table reports the constants defining the nuclear spin Hamiltonian as well as the parameters used to set the gc-M2S sequence in the experiments on 2,3-dibromotiophene presented in fig. S4 (F to H).

Table S3. The table reports the constants defining the nuclear spin Hamiltonian as well as the parameters used to set the gc-M2S sequence in the experiments on Aβ40 presented in Fig. 2B.
Table S4. The table reports parameters used to set the gc-M2S sequence in the experiments on mouse brains presented in Fig. 3.
Materials and methods extended
References (*41*, *42*)

REFERENCES AND NOTES

1. J. Cavanagh, W. J. Fairbrother, A. G. Palmer, M. Rance, N. J. Skelton, *Protein NMR Spectroscopy: Principles and Practice* (Academic Press, ed. 2, 2007).
2. R. W. Brown, Y.-C. Norman Cheng, E. Mark Haacke, M. R. Thompson, R. Venkatesan, *Magnetic Resonance Imaging: Physical Principles and Sequence Design* (John Wiley & Sons Inc., ed. 2, 2014).
3. M. Carravetta, O. G. Johannessen, M. H. Levitt, Beyond the T1 limit: Singlet nuclear spin states in low magnetic fields. *Phys. Rev. Lett.* **92**, 153003 (2004).
4. M. Carravetta, M. H. Levitt, Long-lived nuclear spin states in high-field solution NMR. *J. Am. Chem. Soc.* **126**, 6228–6229 (2004).
5. G. Pileio, Relaxation theory of nuclear singlet states in two spin-1/2 systems. *Prog. Nucl. Magn. Reson. Spectrosc.* **56**, 217–231 (2010).
6. W. S. Warren, E. Jenista, R. T. Branca, X. Chen, Increasing hyperpolarized spin lifetimes through true singlet eigenstates. *Science* **323**, 1711–1714 (2009).
7. P. R. Vasos, A. Comment, R. Sarkar, P. Ahuja, S. Jannin, J. P. Ansermet, J. A. Konter, P. Hautle, B. van den Brandt, G. Bodenhausen, Long-lived states to sustain hyperpolarized magnetization. *Proc. Natl. Acad. Sci. U.S.A.* **106**, 18469–18473 (2009).
8. G. Pileio, M. Carravetta, M. H. Levitt, Storage of nuclear magnetization as long-lived singlet order in low magnetic field. *Proc. Natl. Acad. Sci. U.S.A.* **107**, 17135–17139 (2010).
9. A. Bornet, S. Jannin, G. Bodenhausen, Three-field NMR to preserve hyperpolarized proton magnetization as long-lived states in moderate magnetic fields. *Chem. Phys. Lett.* **512**, 151–154 (2011).
10. G. Stevanato, J. T. Hill-Cousins, P. Håkansson, S. S. Roy, L. J. Brown, R. C. Brown, G. Pileio, M. H. Levitt, A nuclear singlet lifetime of more than one hour in room-temperature solution. *Angew. Chem. Weinheim Bergstr. Ger.* **127**, 3811–3814 (2015).
11. Y. Zhang, P. C. Soon, A. Jerschow, J. W. Canary, Long-lived ^{1}H nuclear spin singlet in dimethyl maleate revealed by addition of thiols. *Angew. Chem. Int. Ed. Eng.* **53**, 3396–3399 (2014).
12. T. Theis, G. X. Ortiz Jr., A. W. J. Logan, K. E. Claytor, Y. Feng, W. P. Huhn, V. Blum, S. J. Malcolmson, E. Y. Chekmenev, Q. Wang, W. S. Warren, Direct and cost-efficient hyperpolarization of long-lived nuclear spin states on universal (15)N2-diazirine molecular tags. *Sci. Adv.* **2**, e1501438 (2016).
13. C. R. Bowers, D. P. Weitekamp, Transformation of symmetrization order to nuclear-spin magnetization by chemical reaction and nuclear magnetic resonance. *Phys. Rev. Lett.* **57**, 2645–2648 (1986).
14. R. W. Adams, J. A. Aguilar, K. D. Atkinson, M. J. Cowley, P. I. P. Elliott, S. B. Duckett, G. G. R. Green, I. G. Khazal, J. Lopez-Serrano, D. C. Williamson, Reversible interactions with para-hydrogen enhance NMR sensitivity by polarization transfer. *Science* **323**, 1708–1711 (2009).
15. J. H. Ardenkjaer-Larsen, B. Fridlund, A. Gram, G. Hansson, L. Hansson, M. H. Lerche, R. Servin, M. Thaning, K. Golman, Increase in signal-to-noise ratio of > 10,000 times in liquid-state NMR. *Proc. Natl. Acad. Sci. U.S.A.* **100**, 10158–10163 (2011).
16. J. Eills, G. Stevanato, C. Bengs, S. Glöggler, S. J. Elliott, J. Alonso-Valdesueiro, G. Pileio, M. H. Levitt, Singlet order conversion and parahydrogen-induced hyperpolarization of ^{13}C nuclei in near-equivalent spin systems. *J. Magn. Reson.* **274**, 163–172 (2017).
17. G. Stevanato, J. Eills, C. Bengs, G. Pileio, A pulse sequence for singlet to heteronuclear magnetization transfer: S2hM. *J. Magn. Reson.* **277**, 169–178 (2017).
18. R. Sarkar, P. R. Vasos, G. Bodenhausen, Singlet-state exchange NMR spectroscopy for the study of very slow dynamic processes. *J. Am. Chem. Soc.* **129**, 328–334 (2007).
19. N. Salvi, R. Buratto, A. Bornet, S. Ulzega, I. Rentero Rebollo, A. Angelini, C. Heinis, G. Bodenhausen, Boosting the sensitivity of ligand-protein screening by NMR of long-lived states. *J. Am. Chem. Soc.* **134**, 11076–11079 (2012).
20. A. Bornet, P. Ahuja, R. Sarkar, L. Fernandes, S. Hadji, S. Y. Lee, A. Haririnia, D. Fushman, G. Bodenhausen, P. R. Vasos, Long-lived states to monitor protein unfolding by proton NMR. *ChemPhysChem* **12**, 2729–2734 (2011).
21. L. Fernandes, C. Guerniou, I. Marín-Montesinos, M. Pons, F. Kateb, P. R. Vasos, Long-lived states in an intrinsically disordered protein domain. *Magn. Reson. Chem.* **51**, 729–733 (2013).
22. S. Mamone, S. Glöggler, Nuclear spin singlet states as magnetic on/off probes in self-assembling systems. *Phys. Chem. Chem. Phys.* **20**, 22463–22467 (2018).
23. P. Saul, S. Mamone, S. Gloggler, Nuclear singlet multimers (NUSIMERs) with long-lived singlet states. *Chem. Sci.* **10**, 413–417 (2019).
24. A. S. Kiryutin, A. N. Pravdivtsev, A. V. Yurkovskaya, H. M. Vieth, K. L. Ivanov, Nuclear spin singlet order selection by adiabatically ramped RF fields. *J. Phys. Chem. B* **120**, 11978–11986 (2016).
25. A. N. Pravdivtsev, A. S. Kiryutin, A. V. Yurkovskaya, H. M. Vieth, K. L. Ivanov, Robust conversion of singlet spin order in coupled spin-1/2 pairs by adiabatically ramped RF-fields. *J. Magn. Reson.* **273**, 56–64 (2016).
26. B. Kharkov, X. Duan, E. S. Tovar, J. W. Canary, A. Jerschow, Singlet excitation in the intermediate magnetic equivalence regime and field-dependent study of singlet-triplet leakage. *Phys. Chem. Chem. Phys.* **21**, 2595–2600 (2019).
27. S. J. Elliott, G. Stevanato, Homonuclear ADAPT: A general preparation route to long-lived nuclear singlet order. *J. Magn. Reson.* **301**, 49–55 (2019).
28. S. J. DeVience, R. L. Walsworth, M. S. Rosen, Preparation of nuclear spin singlet states using spin-lock induced crossing. *Phys. Rev. Lett.* **111**, 173002 (2013).
29. M. C. Tayler, M. H. Levitt, Accessing long-lived nuclear spin order by isotope-induced symmetry breaking. *J. Am. Chem. Soc.* **135**, 2120–2123 (2013).
30. M. H. Levitt, Symmetry constraints on spin dynamics: Application to hyperpolarized NMR. *J. Magn. Reson.* **262**, 91–99 (2016).
31. M. C. D. Tayler, M. H. Levitt, Singlet nuclear magnetic resonance of nearly-equivalent spins. *Phys. Chem. Chem. Phys.* **13**, 5556–5560 (2011).
32. A. Rijal Upadhaya, I. Kosterin, S. Kumar, C. A. von Arnim, H. Yamaguchi, M. Fändrich, J. Walter, D. R. Thal, Biochemical stages of amyloid- peptide aggregation and accumulation in the human brain and their association with symptomatic and pathologically preclinical Alzheimer's disease. *Brain* **137**, 887–903 (2014).
33. N. Rezaei-Ghaleh, S. Kumar, J. Walter, M. Zweckstetter, Phosphorylation interferes with maturation of amyloid-β fibrillar structure in the N terminus. *J. Biol. Chem.* **291**, 16059–16067 (2016).
34. N. Rezaei-Ghaleh, M. Amininasab, K. Giller, S. Kumar, A. Stündl, A. Schneider, S. Becker, J. Walter, M. Zweckstetter, Turn plasticity distinguishes different modes of amyloid-β aggregation. *J. Am. Chem. Soc.* **136**, 4913–4919 (2014).
35. Y. Xiao, B. Ma, D. McElheny, S. Parthasarathy, F. Long, M. Hoshi, R. Nussinov, Y. Ishii, Aβ(1–42) fibril structure illuminates self-recognition and replication of amyloid in Alzheimer's disease. *Nat. Struct. Mol. Biol.* **22**, 499–505 (2015).
36. J. Shen, in *Magnetic Resonance Spectroscopy*, C. Stagg, D. Rothman, Eds. (Academic Press, 2014), pp. 111–121.
37. J. R. Moffett, B. Ross, P. Arun, C. N. Madhavarao, A. M. A. Namboodiri, *N*-Acetylaspartate in the CNS: From neurodiagnostics to neurobiology. *Prog. Neurobiol.* **81**, 89–131 (2007).
38. I. Tkáč, G. Oz, G. Adriany, K. Ugurbil, R. Gruetter, In vivo 1H NMR spectroscopy of the human brain at high magnetic fields: Metabolite quantification at 4T vs. 7T. *Magn. Reson. Med.* **62**, 868–879 (2009).
39. S. J. Devience, R. L. Walsworth, M. S. Rosen, Nuclear spin singlet states as a contrast mechanism for NMR spectroscopy. *NMR Biomed.* **26**, 1204–1212 (2013).
40. V. Govindaraju, K. Young, A. A. Maudsley, Proton NMR chemical shifts and coupling constants for brain metabolites. *NMR Biomed.* **13**, 129–153 (2000).
41. C. Bengs, M. H. Levitt, SpinDynamica: Symbolic and numerical magnetic resonance in a Mathematica environment. *Magn. Reson. Chem.* **56**, 374–414 (2018).
42. Wolfram Mathematica 11.3 (Wolfram Research Incorporation, 2018).

Acknowledgments: K. Overkamp is acknowledged for the chemical synthesis of the Aβ peptide. P. Saul is acknowledged for the preparation of the AGG tripeptide sample doped with Gd(III). **Funding:** S.G. acknowledges funding by the Max Planck Society and the Max Planck Institute for Biophysical Chemistry. N.R.-G.'s research was supported by a German Research Foundation (DFG) grant (grant no. RE3655/2-1). **Author contributions:** S.M. designed the gc-M2S sequence and performed the theoretical analysis and the supporting simulations. N.R.-G. and S.M. developed the singlet-filtered TOCSY sequence. S.M., N.R.-G., and S.G. designed the experiments. F.O. prepared the ex vivo brains. S.M. and N.R.-G. conducted NMR experiments. S.G. envisioned the scheme for general and versatile singlet state experiments. All authors discussed the experimental results and analyses. S.M., S.G., and N.R.-G. wrote the paper. **Competing interests:** The authors declare that they have no competing interests. **Data and materials availability:** All data needed to evaluate the conclusions in the paper are present in the paper and/or the Supplementary Materials. Additional data related to this paper may be requested from the authors.

Submitted 20 August 2019
Accepted 4 December 2019
Published 21 February 2020
10.1126/sciadv.aaz1955

Citation: S. Mamone, N. Rezaei-Ghaleh, F. Opazo, C. Griesinger, S. Glöggler, Singlet-filtered NMR spectroscopy. *Sci. Adv.* **6**, eaaz1955 (2020).